

VERIFICATION OF TURBULENT CORRELATION AND IMPACT STUDY OF HIGH-PRESSURE ABRASIVE WATER JET

Can Kang
Jiangsu University,
Zhenjiang, Jiangsu Province, China

Haixia Liu, Minguang Yang
Jiangsu University
Zhenjiang, Jiangsu Province, China

ABSTRACT

At 260 MPa, a high-pressure waterjet are investigated by utilizing phase Doppler anemometry (PDA) technique. The sectional distributions of average velocity and root-mean-square velocity in the jet stream are acquired and discussed. Jet-cutting experiment is conducted with Ti6Al4V plates serving as the target samples. Stand-off distance (SOD) and the relative angle between jet direction and target surface are emphasized. The morphological characteristics on the cut surfaces are visualized by utilizing a scanning electron microscope (SEM) and an optical profiling instrument. It is proved that the high-velocity jet core plays a significant role in terms of the energy concentration and velocity magnitude. The behavior of the abrasive particles is inevitably affected by the surrounding water. The grooves of diverse profiles on the cut surface are highly associated with the radial expansion of the jet stream when the jet develops downstream. Furthermore, the complicated abrasive particle's behavior is one of the decisive factors affecting the roughness of the cut surface. The results also indicate that there exists an optimal position of inclined sample plate corresponding to the combination of operation parameters in this experiment.

1. INTRODUCTION

Abrasive waterjet (AWJ) has been successfully used in many manufacturing processes as a reliable technique. The operation performance of high-pressure abrasive water-jet system has been improved continuously in recent years. According to the empirical predictions, the average jet velocity at the outlet of the nozzle can be as high as 700 m/s at the jet pressure of 300 MPa, which is rather scarce in the field of liquid flow. Although the maximum achievable operation pressure of a high-pressure generator has been enhanced remarkably in recent years, the fluid dynamics phenomena inside the tiny multiphase jet stream have not been enumerated and elucidated yet. If cavitation and compressibility effects are additionally taken into account, the study of abrasive water jet will pose a big challenge to existing research methods [1].

Waterjet is seemingly an easy-to-handle subject with simple boundary conditions. However, various difficulties in treating the jet flow have been encountered in both experimental and numerical studies. Especially under high-pressure conditions, there are several small-scale phenomena such as disturbance of surrounding air on the jet stream, breakup of the jet stream along the jet direction, and turbulent fluctuations that cannot be accurately modeled with current physical and mathematical methods. In terms of numerical model, lots of efforts have been devoted to developing more reasonable models such as droplet–droplet collision model, Eulerian-Lagrangian model, etc. It is also proved in the myriad of recently published reports that liquid jet breakup and droplet distribution are being specifically focused on [2]. Regarding the high-pressure waterjet used to cut metal workpieces, the fluid is seemingly concentrated into a tiny stream, the corresponding fluid dynamics phenomena need to be further probed as well. Among those studies of the high-pressure waterjet flow field, the turbulent characteristics inside the jet stream have been rarely demonstrated by using reliable data [3].

In this paper, the fluid dynamics analysis is conducted on the basis of measured velocity distributions in a jet stream section. The non-intrusive flow measurement technique of phase Doppler anemometry is utilized to detect the tiny jet stream. Then the jet-cutting experiment is carried out with Ti6Al4V plate being used as the target sample. Stand-off distance and the inclination angle of the target plate are two operation parameters that are specifically investigated in the experiment. For the cut surfaces, morphological features are examined by using a scanning electron microscope and an optical profiling instrument. Thus the relationship between the behavior of abrasive particles and the traces on the cut surface is expected to be demonstrated.

2. FLOW MEASUREMENT

As shown in Fig.1, an ultra-high-pressure jet-cutting system was used in the experiment. The rated power consumption of the system is 30 kW and available maximum water flow rate is $6.167 \times 10^{-5} \text{ m}^3/\text{s}$. The maximum jet pressure of 380 MPa can be achieved with the system and the

jet pressure of 260 MPa was adopted here. With respect to the liquid-solid two-phase flow emanating from an AWJ nozzle, there are several problems in the flow measurement that have not been well treated. One is that the inevitable overlapping among abrasive particles will confuse the general image-processing algorithms and the other lies in that the laser cannot penetrate the abrasive particles and consequently the flow behind the abrasive particles will not be detected. In recent study, shadowgraphy technique was relied on to measure the size and velocity of abrasive particles. The study was carried out on the air-abrasive two-phase jet and the acquired maximum abrasive velocity exceeded 100 m/s. When high-speed abrasive particles passed through the space between two mask plates, the shadowgraphy images were captured by using high-speed camera and pulsated laser light [4]. Both the size and velocity of abrasive particle can be obtained with this method. However, the method is impracticable in terms of its application in the water. Therefore the measurement in this study was conducted with pure water as the jet medium. With equivalent jet pressure, the data acquired in pure water is expected to be connected to those kinetic parameters of abrasive particle.

A Dantec PDA system was used to measure the velocity distributions inside the jet stream. PDA technique has been extensively and successfully applied to acquire the transient velocity fluctuations inside the water jet at a wide range of jet pressures [5]. The two jet sections investigated (denoted by $Z=3.0$ mm and $Z=6.0$ mm) are 3.0 mm and 6.0 mm from the nozzle outlet section, respectively. The $Z=3.0$ mm section is representative for its being generally adopted in actual jet-cutting operations. Before the PDA measurement, a high-speed camera is used to capture the transient variation of the jet stream profile. Three typical images are shown in Fig.2 where the time interval between every two neighboring images is 1 ms. The bottom section of the jet segment shown in the images is 3.0 mm from the nozzle outlet. As can be found from Fig.2, the jet stream is concentrated into a tiny jet stream except that the interface between jet fluid and surrounding air fluctuates to some extent. Those bubble-like patterns in the images of jet stream imply the disturbance of surrounding air on the outer edge of the jet stream. Along the jet segment displayed, the diameter of the jet stream can be deemed as invariant. Therefore, the PDA measurement of the section 3.0 mm from the nozzle outlet well embodies the features of the concentrated part of the jet stream.

For such a high velocity magnitude, uncertainties for the averaged velocities were estimated to be 10-15%, which came dominantly from systematic errors. The placement of measurement volumes on investigated section is schematically shown in Fig.3(a). A validation test was carried out before the data-recording process, with the optical focus adjusted to be approximately at the center of the jet stream (the actual center can only be pinpointed through the experimental results). There were over 2000 particles captured within the time interval of 60 ms, as is shown in Fig.3(b). Since no additional seeding particles were added into the water beforehand, the inherent impurity particles inside the water were used as seeding particles, as was proved to be effective by the comparison among the results obtained through repeating the validation process.

3. DISCUSSION OF TURBULENT FLOW PARAMETERS

The average velocity at each measurement volume is obtained by averaging the single fluid particle' velocity values, which is in accordance with the concept of average velocity in the field of engineering turbulence [6]. As shown in Fig.4(a), at the $Z=3.0$ mm section, there is a rather flat average velocity distribution near the center of the jet stream and the maximum velocity exceeds 570 m/s. The central part of the $Z=3.0$ mm section is conceived to be within the range of the well-recognized jet-core zone. If this velocity distribution of water is completely transferred to the abrasive particles passing through the same section, with the physical properties of abrasive particles being considered, the amount of the kinetic energy carried by the abrasive particles will be quite remarkable. As for the $Z=6.0$ mm section, the overall magnitude of average velocity is reduced and the distribution indicates the obvious expansion of the jet stream within such a small distance of development from the $Z=3.0$ mm section.

Turbulence is featured by vortices of various scales and turbulent fluctuations. By using PDA technique, detailed velocity information in each measurement volume can be recorded within a rather short time-span. Consequently, the distributions of root-mean-square velocity can be deduced with the aid of statistical methods. Root-mean-square velocity is usually applied to explain the turbulent fluctuations in the turbulent jet flow. The distributions of root-mean-square velocity on the two studied sections are shown in Fig.4(b). Apparently, the overall magnitude of root-mean-square velocity on the $Z=3.0$ mm section is smaller than its counterpart on the $Z=6.0$ mm section. Furthermore, the sparse distribution points on the section of $Z=6.0$ mm reasonably reflect the disturbance on the jet stream by the surrounding air. Regarding the actual jet-cutting operation, small velocity fluctuations is expected to influence the surface quality positively. Concurrently, with the expansion of the jet stream, the radial velocity component of the jet fluid will lead to the deterioration of the surface roughness to some extent. Although the fluctuations in pure-water jet and water-abrasive two-phase jet are essentially different, the transient behavior of abrasive particle will be undoubtedly driven by the surrounding water.

4. JET-CUTTING EXPERIMENT

The mixing of abrasive particles and water in the inner passage of jet nozzle cannot be visualized and explained in detail with existing methods. However, the traces on the processed material surface can explain the influence of the water-abrasive jet indirectly. The same jet pressure of 260 MPa was employed in the jet-cutting experiment. Abrasive's physical properties have a non-negligible effect on the surface quality obtained [7]. The high-hardness garnet particles with equivalent diameter of 0.25 mm were used in the experiment. The shapes of the particles are considerably irregular, as would further improve the grinding and cutting effects. The edges and corners of abrasive particles are always the research focus due to their complexity and diversity in actual applications. The impact of irregular particles on target surface has been simulated with

smoothed particle hydrodynamics (SPH) model. In that study, the initial velocity of the particles is 105 m/s and the dimensions of the target area are 600 μm ×600 μm . The material-removing process was illustrated under various conditions of abrasive particle's incident angles [8]. The impact of abrasive particles on the target metal plate has also been simulated with the commercial LS-DYNA code package. The velocity of abrasive particle is proved to have a dominant influence on the development of the von Mises stress inside the target plate during the impact process [9].

Ti6Al4V plate with a uniform thickness of 2.56 mm was used as the target sample here. The traversing speed of the nozzle was set to be 5 mm/s. Ti6Al4V alloy is characterized by high specific strength and relatively low density at normal pressure and temperature. The machinability of Ti6Al4V is poor due to its mechanical and physical properties. Abrasive water jet has been proved to be a flexible machining method for Ti6Al4V in several studies. In the experiment, stand-off distance and incident angle are two major concerns which are necessarily related to the resultant morphological features on the cut surface. The relative angle between jet stream and target surface was produced by adjusting the position of the target surface while the jet direction was kept invariant.

5. SURFACE QUALITY

5.1 Influence of stand-off distance on cut surface

As a crucial parameter, stand-off distance is usually modulated according to the material property and the dimensions of the sample. Different stand-off distances will lead to ultimately different morphological features on the cut surface, as is linked to several factors such as nozzle's traverse speed, jet pressure, abrasives, etc. Fig.5 contains four images of the cut surfaces obtained by utilizing a scanning electron microscope at stand-off distances of 1.8 mm, 3.4 mm, 4.7 mm and 6.2 mm, respectively. The four images were acquired when the jet direction was made to be perpendicular to the target surface.

Even at the smallest stand-off distance of 1.8 mm, the traces left by the abrasive particles are apparent with such a small-scale observation manner. The overall direction of the traces is uniformly vertical. With the increase of stand-off distance, the irregular grooves with various widths on the cut surface turn out to be visible. The deviation of the overall direction of the grooves from vertical direction becomes more salient at large stand-off distances, as denotes that although the kinetic energy of the abrasive particles is still sufficient to cut through the Ti6Al4V plate, the time consumed to finish such a process will increase with a constant traverse speed of the nozzle. At the stand-off distance of 4.7 mm, there are two distinct horizontal grooves that truncate other vertical grooves. The width of the upper horizontal groove is nearly 20 μm . The reasons for such a kind of morphological feature are diverse. The most immediate reason may lie

in that the motion of abrasive particles is made to deviate from their original vertical direction by the collision among particles.

There are two factors that should be noticed and will inevitably make the process more sophisticated. One is that the edges and corners of the abrasive particles play a significant role in cutting through the sample and leaving irregular traces on the cut surface. The other factor is that the abrasive particles may be shattered after the intensive action with the Ti6Al4V plate. The fragment particles will still be active in the narrow crevice. The two factors cannot be explained in-depth with available experimental methods. Besides that, some abrasive particles may be embedded into the cut surface due to the radial velocity component or insufficient energy, which is a more troublesome problem for physically modeling such a jet-cutting process.

5.2 Influence of inclination angle on the cut surface

In order to accomplish a continuous cut process with the jet's cut-through capability and stand-off distance being jointly taken into account, a supporting base shown in Fig.6 was designed and the inclination angle of α could be adjusted in the range of 5° to 45° . Consequently, when the Ti6Al4V plate was placed onto the supporting base, the relative angle between the plate surface and jet direction could be varied at different values of α , as is shown in Fig.6. Furthermore, during the jet-cutting process, with the traversing of the nozzle, the abrasive water jet continuously impacted the target plate, as was accompanied by the variation of stand-off distance. The critical position before which the plate was cut through would unavoidably appear during such a jet-cutting process.

Four inclination angles of 10° , 15° , 20° and 25° were investigated in the experiment. At each inclination angle, the maximum cut-through length s , as shown in Fig.6, and the corresponding stand-off distance were firstly measured after the jet-cutting process. The results are shown in Fig.7. With the increase of inclination angle, the maximum cut-through length decreases, as is seemingly understandable because the stand-off distance increases most rapidly at the largest inclination angle of 25° . However, the maximum stand-off distance corresponding to the position where maximum cut-through length occurs at the inclination angle of 15° . It means that the optimal inclination angle does not always be the smallest one, which is greatly dependent on the behavior of abrasive particles in the jet stream.

The cut surfaces obtained at the inclination angles of 10° and 15° are chose to be further examined in this study. The cut surface's roughness is quantitatively measured with an optical profiling instrument. Since the observed area must be limited to be compatible with the available scanning resolution. The dimensions of the observed area were set to be $0.90\text{ mm}\times 1.25\text{ mm}$. With the optical profiling instrument utilized, the maximum surface roughness could also be acquired for a certain observed area.

Figure.8 contains the surface profiles at the inclination angle of 10° . In these figures, the traversing direction of the nozzle is uniformly from left to right. The acquired surface roughness decreases with the movement of the nozzle. In Figs.8(1a) and (1b), the values of the maximum surface roughness are $154.78 \mu\text{m}$ and $221.37 \mu\text{m}$, respectively. However, the overall distribution of surface roughness is rather uniform for such a machining method. In Figs.8(3a) to (4b), the surface quality can be deemed as invariant with the increase of stand-off distance.

The contours of surface roughness at the inclination angle of 15° are displayed in Fig.9. In Figs.9(1a) and (1b), the values of maximum surface roughness are $137.39 \mu\text{m}$ and $117.18\mu\text{m}$, respectively. For such an inclination angle, the surface quality at smaller stand-off distance is not always better. Clear discrepancy on the cut surface is found in Figs.9(2a) to (3b), where the variation of surface roughness along the cutting route turns out to be quite irregular. Although the sampling process cannot encompass the entire scope of the cut surface, it serves as a reasonable comparison between the results obtained separately at the two different inclination angles. Since the maximum cut-through length at the inclination angle of 15° is smaller than that at inclination angle of 10° , the examined zones in Fig.9 are accordingly less than that in Fig.8.

The surface roughness can also be demonstrated in the manner of distribution curve, as is shown in Fig.10. Those curves correspond to the variation of surface roughness along the routes parallel to the nozzle's traverse direction. In Fig.10(a), the nearly linear variation of surface roughness along the selected route well explains the energy attenuation with the continuous increase of stand-off distance. The fluctuations of surface roughness at the inclination angle of 15° , as shown in Fig.10(b), are consistent with the results in Fig.9.

In this analysis, the impact of water droplet on target plate is not taken into account because the effect of water is hardly comparable with that of abrasive particles, as is an acceptable viewpoint in most studies of abrasive waterjet. However, in terms of the complex effects such as cavitation and compressibility, both the two-phase turbulent flow and the compound impact on the target surface deserve a deterministic explanation [10].

6. CONCLUSIONS

(1) The velocity distributions obtained by using PDA well indicate the kinetic energy distribution and turbulent characteristics in the jet stream, as strongly supports the powerful impact effect of the abrasive particles through the inherent connection between the water and abrasive particles in high-pressure abrasive waterjet.

(2) The behavior of abrasive particles is decisive for the resultant morphological features on the cut surface. Besides the influence of the irregular shapes of the abrasive particles, the stand-off distance contributes to the various traces on the resultant surface as well.

(3) The maximum cut-through length achieved is reduced when the inclination angle increases. However, the maximum stand-off distance corresponding to the maximum cut-through length occurs at the inclination angle of 15° , which is not the smallest one. Qualitative distribution of surface roughness is proved to be an effective manner of expressing the surface quality on Ti6Al4V surface.

7. ACKNOWLEDGMENTS

The authors are grateful to the Natural Science Foundation of China (Grant Nos. 51205171 and 50806031), the Jiangsu Overseas Research and Training Program for University Prominent Young and Middle-aged Teachers and Presidents, and the Science Foundation for Post-doctorate Research from Jiangsu Province of China (Grant No.1201026B).

8. REFERENCE

- [1] YANG Minguan, WANG Yuli, KANG Can. Cavitation and Wear in the Micro Jewel Nozzles of Ultra-high Pressure Water Jet. *Chinese Journal of high pressure physics* 24(2010) 286–292.
- [2] S.S. Yoon, J.C. Hewson, P.E. DesJardin, D.J. Glaze, A.R. Black, R.R. Skaggs. Numerical modeling and experimental measurements of a high speed solid-cone water spray for use in fire suppression applications. *International Journal of Multiphase Flow* 30 (2004) 1369–1388.
- [3] WANG Yu-Li, YANG Min-Guan, KANG Can, YU Feng. Structure of Ultra-high Pressure Water Jet within 400 MPa. *Journal of Engineering Thermophysics* 31(2010) 959–962.
- [4] D. Dehnadfar, J. Friedman, M. Papini. Laser Shadowgraphy Measurements of Abrasive Particle Spatial, Size and Velocity Distributions Through Micro-masks Used in Abrasive jet Micro-machining. *Journal of Materials Processing Technology* 212 (2012) 137–149.
- [5] KANG Can, WANG Wei-feng, ZHANG Feng, YANG Min-guan. Experiment Study of Fan Free Water Jet Flow by Using PDPA. *Journal of Hydrodynamics* 25(2010) 822–829.
- [6] KANG Can, YANG Min-Guan, Zhang Feng, Gao Bo. Energy Distribution and Statistic Characteristics in Round Water Jet. *Journal of Drainage and Irrigation Machinery Engineering* 29(2011) 160–164.
- [7] M.Gent, M.Menéndez, S.Torno, J.Toraño, A. Schenk. Experimental Evaluation of the Physical Properties Required of Abrasives for Optimizing Waterjet Cutting of Ductile Materials. *Wear* 284- 285 (2012) 43–51.
- [8] M. Takaffoli, M. Papini. Numerical Simulation of Solid Particle Impacts on Al6061-T6 Part II: Materials Removal Mechanisms for Impact of Multiple Angular Particles. *Wear* 296 (2012) 648–655.
- [9] Kang Can, Zhou Liang, Wang Yuli, Gong Chen. Simulation and Experiment of Impinged Material Surface with Abrasive Water Jet. *Journal of Jiangsu University (Natural Science Edition)* 34(2013) 276–280.
- [10] M.B.Lesser. The Impact of Compressible Liquids. *Annual Review of Fluid Mechanics* 15(1983) 97–122.

9. FIGURES

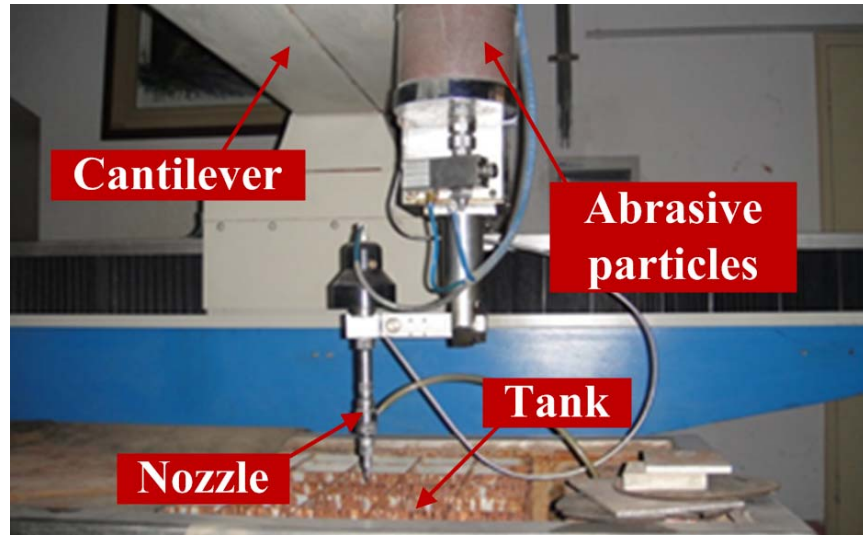


Figure 1. High-pressure system used in the experiment

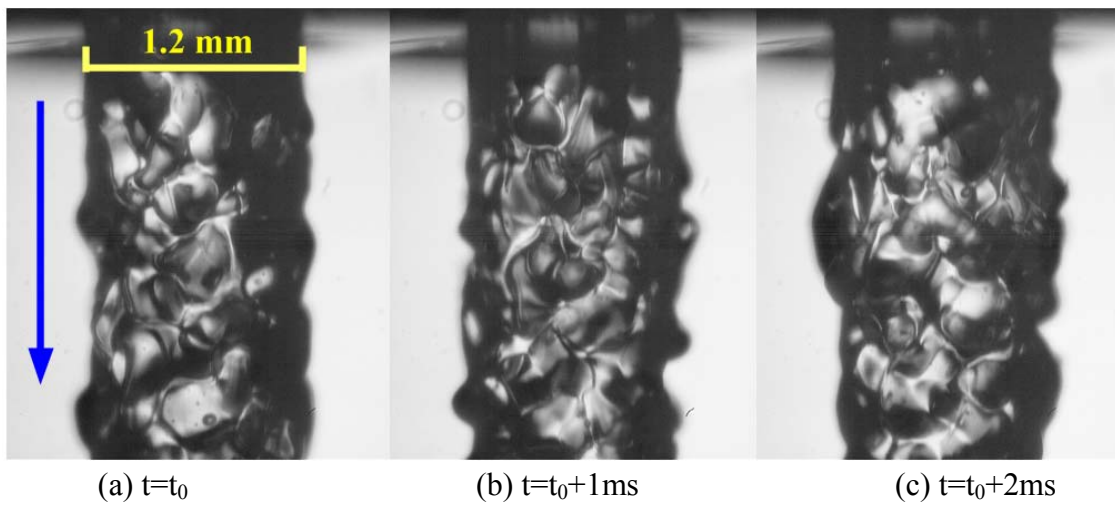
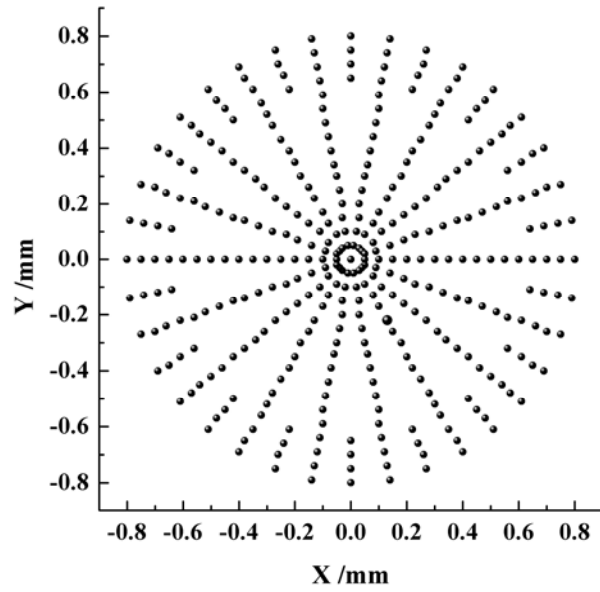
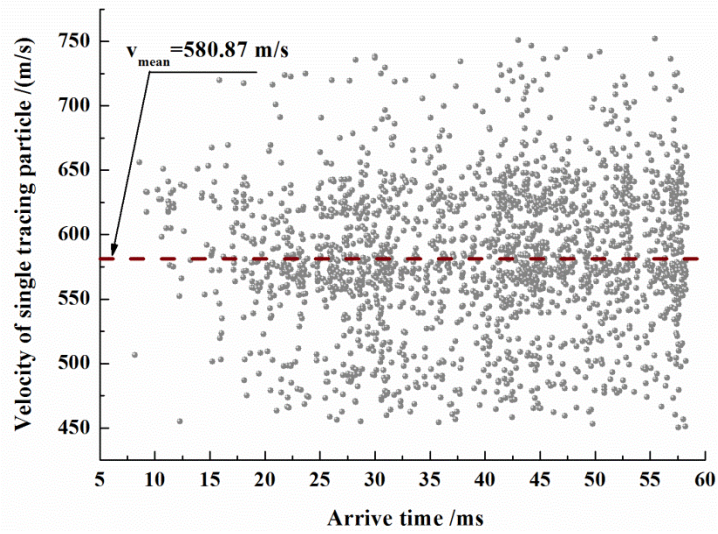


Figure 2. Transient jet stream profiles obtained by using high-speed photography technique

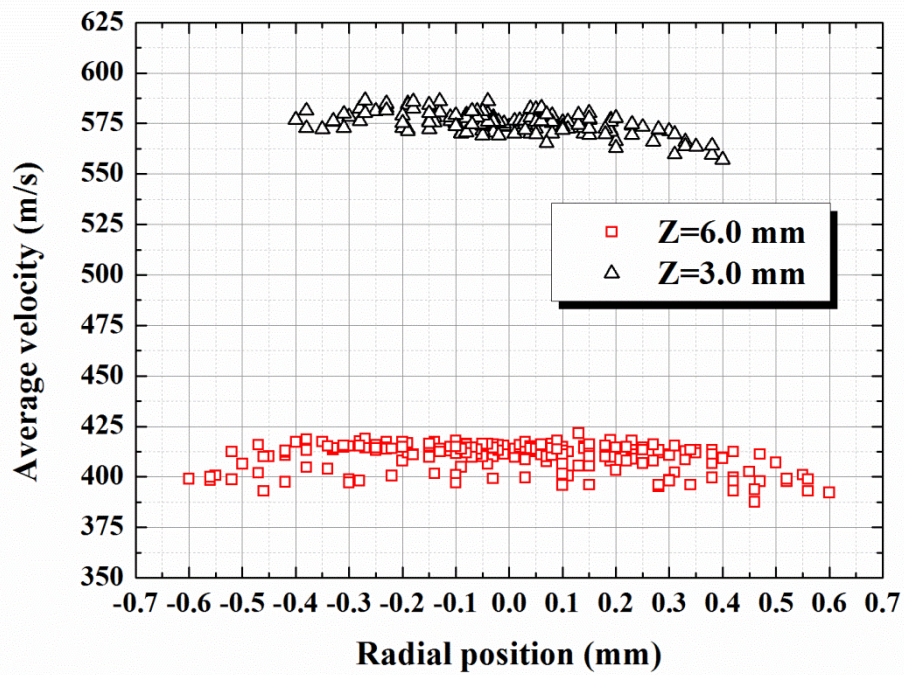


(a) Placement of measurement points

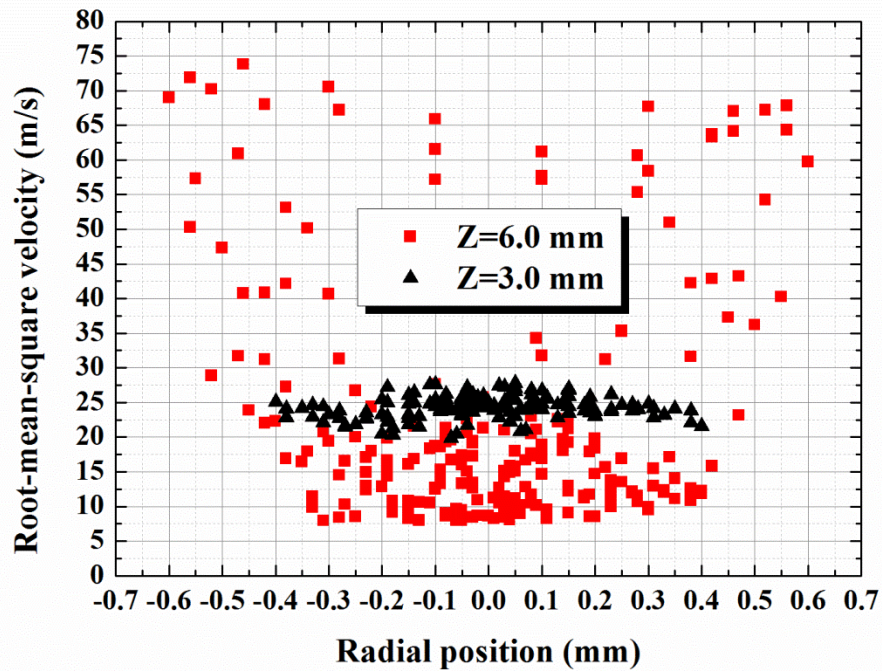


(b) Monitoring of points at the same position

Figure 3. Distribution of sampling points on a jet stream section and validation of the PDA sampling process



(a) Average velocity distribution



(b) Root-mean-square velocity distribution

Figure 4. Velocity distributions on the two sections of 3.0 mm and 6.0 mm from the nozzle outlet, respectively

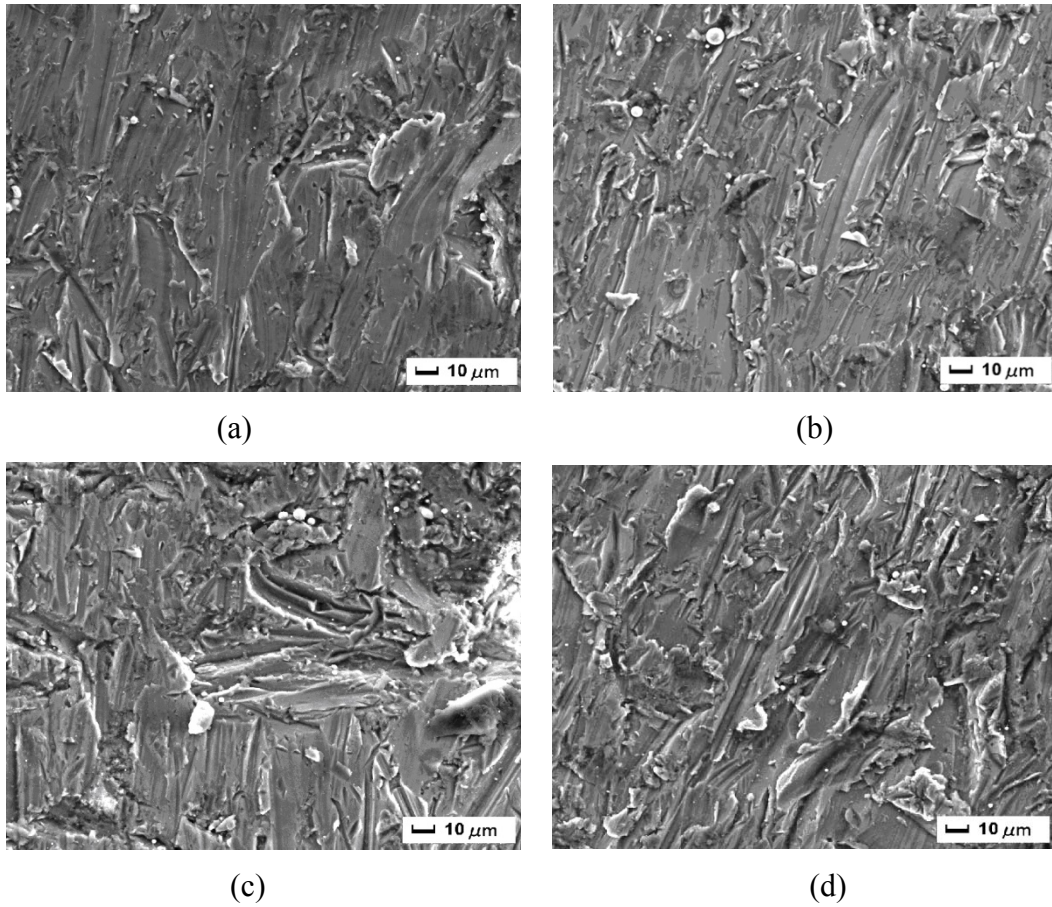


Figure 5. SEM images of cut surfaces at various stand-off distances

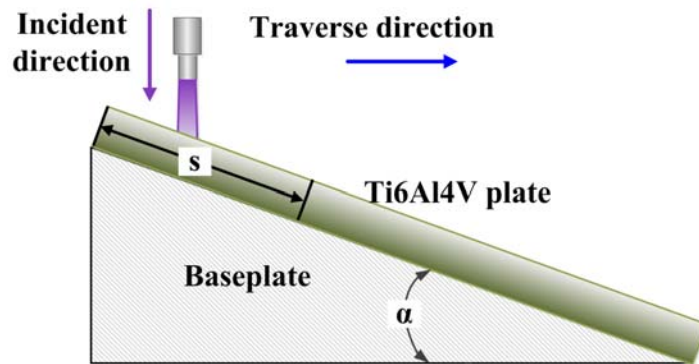


Figure 6. Experiment scheme of jet-cutting with inclined sample plate

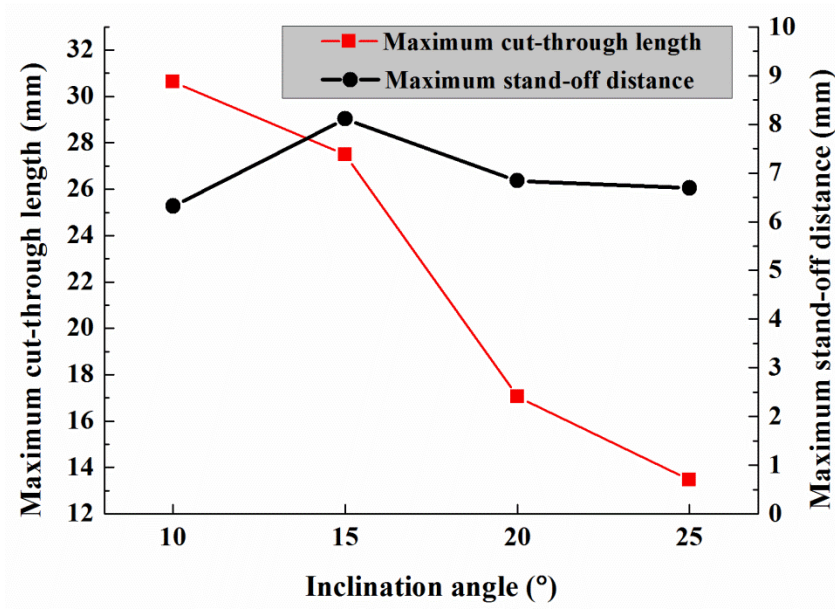
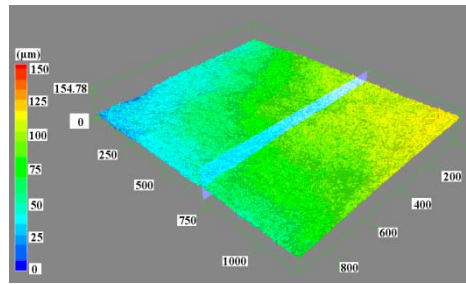
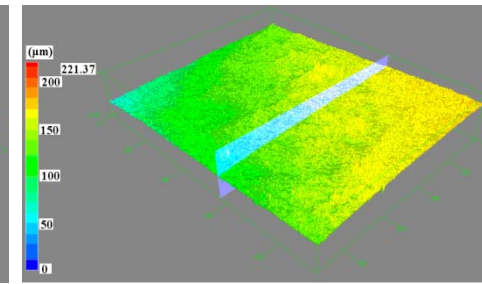


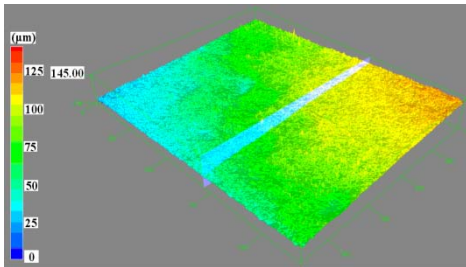
Figure 7. Cut-through parameters at different inclination angles



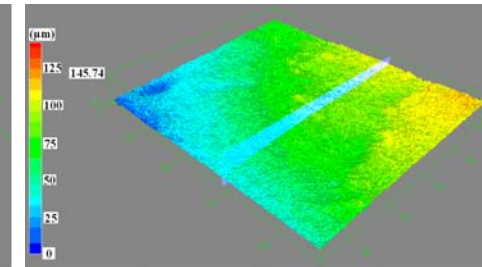
(1a)



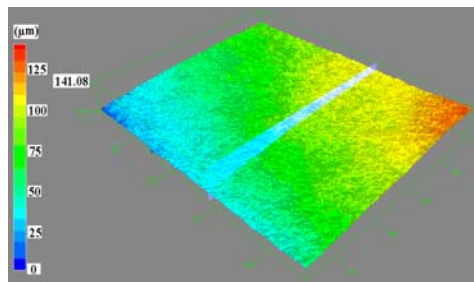
(1b)



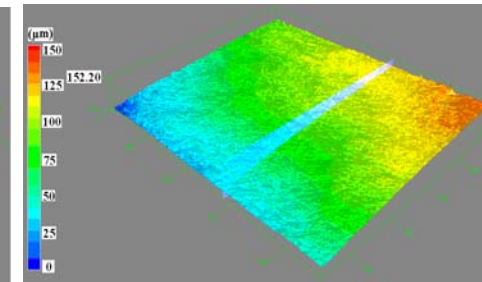
(2a)



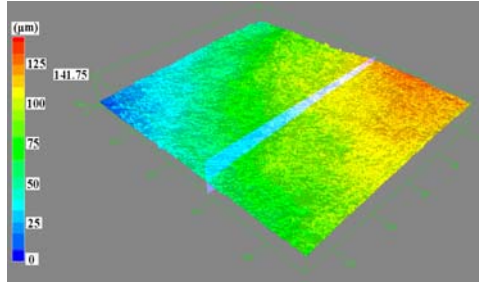
(2b)



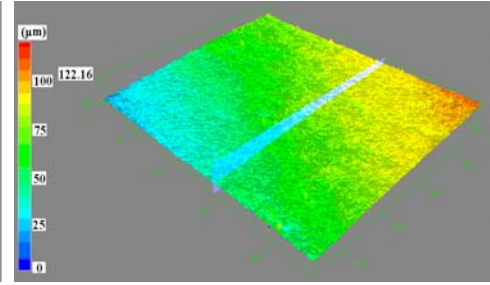
(3a)



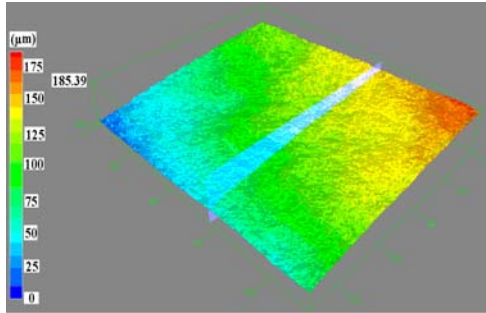
(3b)



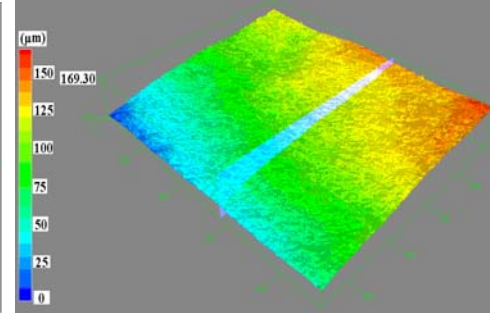
(4a)



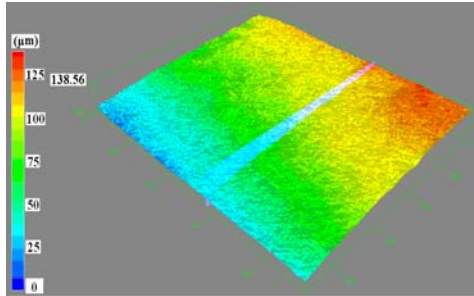
(4b)



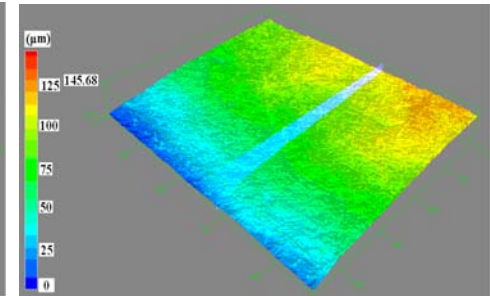
(5a)



(5b)

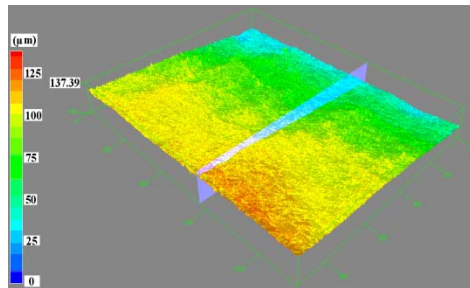


(6a)

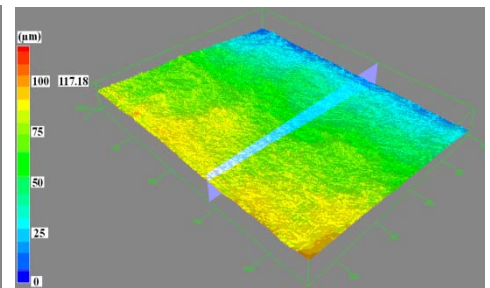


(6b)

Figure 8. Surface morphological profiles at incident angle of 10°



(1a)



(1b)

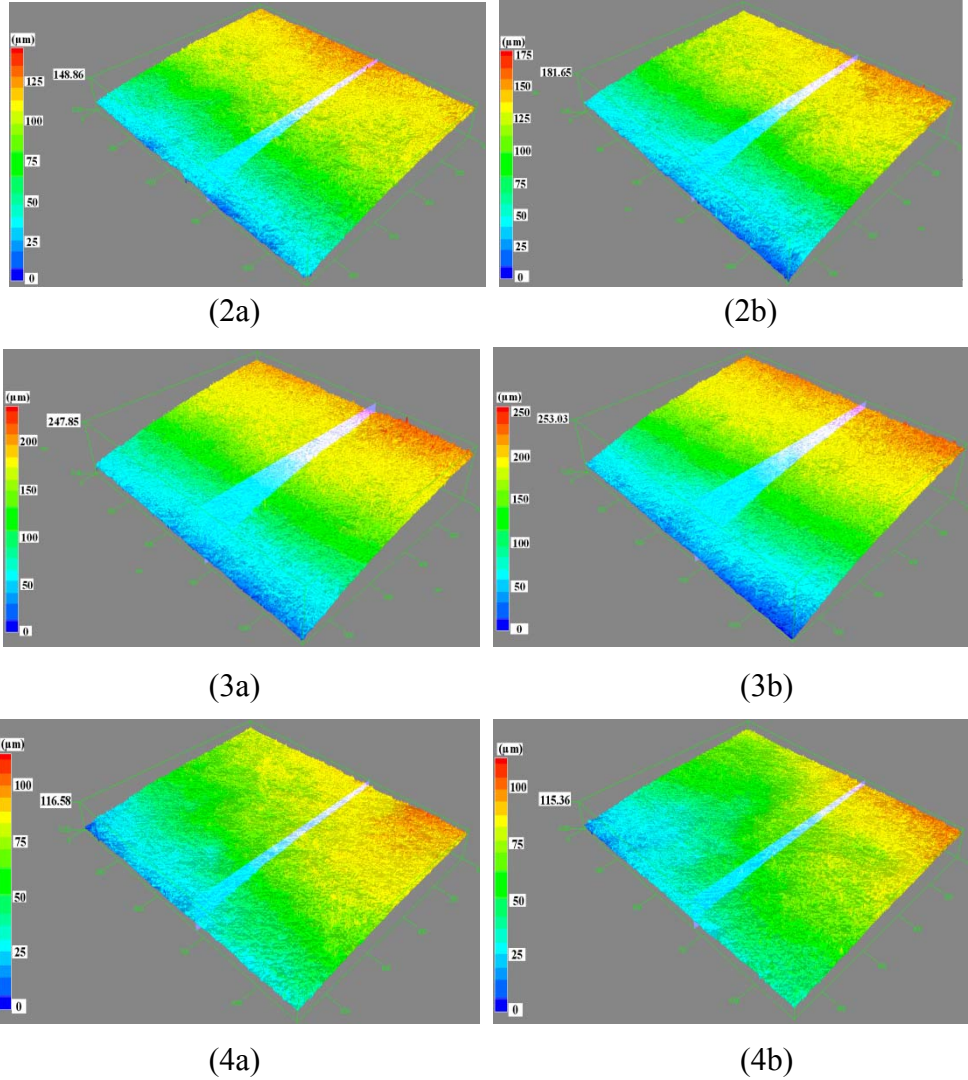
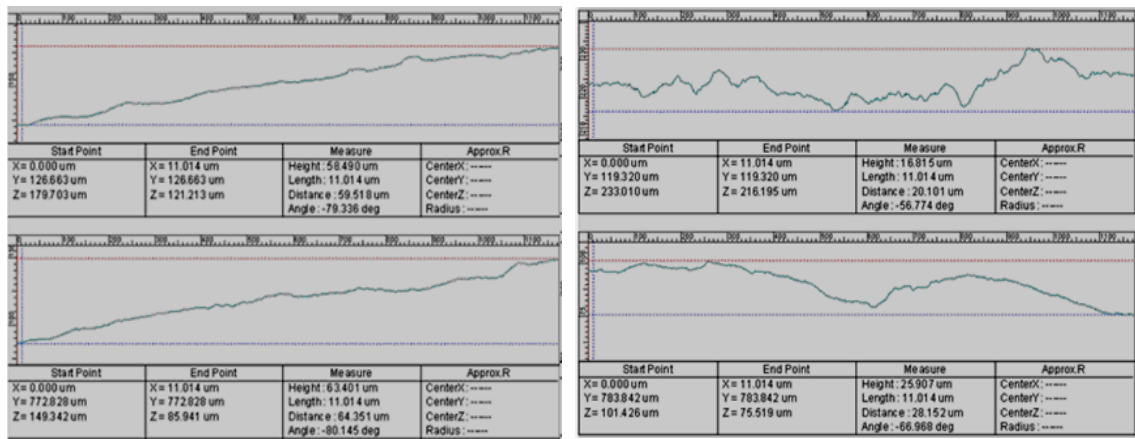


Figure 9. Surface morphological profiles at incident angle of 15°



(a) Inclination angle of 10°

(b) Inclination angle of 15°

Figure 10. Surface roughness at different incident angles